Chapter 2 Synthesis of Polycrystalline and Single-Crystal Growth of $BaFe_{12}O_{19}$

2.1 Introduction

This study deals with the exploration of new magnetic and non-magnetic phase transitions in $BaFe_{12}O_{19}$ (BFO) in the 1.5 K to 200 K temperature range. In this study, both single crystals and powder samples of BFO have been investigated. In this chapter, the details of synthesis of BFO powders and growth of single crystals are presented along with characterization of their composition and crystal structure. BFO powders in the past have been synthesised using several different techniques: solid state thermochemical reaction [165–167], sol-gel [168–171], coprecipitation [168,172–174] and hydrothermal [175–177]. Similarly, single crystals of BFO have been grown using flux method [178,179] and directly from melt without any flux [15]. We here synthesised BFO powder using conventional solid-state thermochemical reaction method [165–167]. The synthesis of monophasic BFO is challenging because of the formation of an unwanted phase like $BaFe_2O_4$ and presence of unreacted ingredients like Fe_2O_3 and BaO during the synthesis [180–182]. To avoid the formation of the impurity phases and hence unreacted ingredients, the calcination and sintering temperatures and time play very important role. We have grown single crystals of BFO using high-temperature flux method [178,179]. The phase purity of powder was verified using X-ray diffraction at various stages of the synthesis during calcination and sintering stages. The orientation and phase purity of single crystals of BFO were checked by single-crystal Laue diffraction and powder diffraction techniques. Ba and Fe stoichiometry was verified using energy dispersive X-ray spectroscopy while oxygen content was determined using iodometry [183–185].

2.2 Experimental

The phase purity of the synthesized samples was checked using X-ray diffraction (XRD) method. The power XRD measurements were carried out using a high resolution 18-kW Cu rotating anode powder diffractometer fitted with curved crystal graphite monochromator in the diffracted beam (Rigaku, model no. RINT 2500/PC series). The diffractometer operates in the Bragg-Brentano geometry. The XRD data were collected on the annealed powders of the calcined and sintered samples in the 2θ range 20 to 70 degrees at a step of 0.02 with a scan rate of 3^0 per min. Rietveld and Lebail refinements were carried out using FullProf suite [186]. The Laue diffraction patterns were recorded in the transmittance geometry using polychromatic beams collimated along the c-axis of the single crystals of BFO.

Ba and Fe contents in the single-crystals was verified Energy Dispersive X-ray spectroscopy (EDX) (Oxford, model no. 51-ADD0048) attachment fitted in the Scanning Electron Microscope (SEM) (Zeiss, model no. EVO 18). The oxygen content was determined using iodometry technique.

For neutron powder diffraction (NPD) measurements, the sintered pellets of $BaF_{12}O_{19}$ (BFO) were crushed into fine powders using mortar pastel. The crushed powder was annealed at 873 K for 10 hours. The room temperature NPD patterns was recorded for such annealed powder samples at a wavelength of 0.207150Å using high-resolution powder diffractometer SPODI at FRM II, Garching, Germany [187,188].

2.3 Synthesis of $BaFe_{12}O_{19}$ Polycrystalline Samples

For the synthesis of barium hexaferrite polycrystalline samples by solid state thermochemical reaction route, analytical reagent grade chemicals: $BaCO_3$ (≥ 99.0% assay, Sigma Aldrich) and Fe_2O_3 (≥ 99.0% assay, Sigma Aldrich) were used. The different steps involved in the synthesis of powder samples is presented in the following.

2.3.1 Optimization of Calcination Temperature

The ingredients, Fe_2O_3 and $BaCO_2$, in stoichiometric ratio were first mixed using an agate mortar and pestle for 3 hours using acetone as mixing medium. The mixed powder was ball milled in a zirconia jar using zirconia balls as the grinding medium and acetone as the milling medium on a planetary ball mill for 12 hours. After 12 hours the mixture was dried at room temperature. After drying, samples were calcined in alumina crucibles at two different temperatures 1273 K and 1373 K for 6 hours. The calcined sample was crushed to fine powders using mortar and pestle and annealed for 10 hours at 873 K before checking the phase purity. The XRD pattern recorded on such annealed calcined samples are shown in Fig. 2.1. A careful comparison of this XRD profile with that reported in the literature [182] suggest that at 1273 K all the peak expected one are due to the hexagonal phase of BFO. However, there is an impurity peak marked with an asterisk (*) in Fig. 2.1 due to the presence of unreacted Fe_2O_3. At 1373 K, this peak disappears and sample is now monophasic.

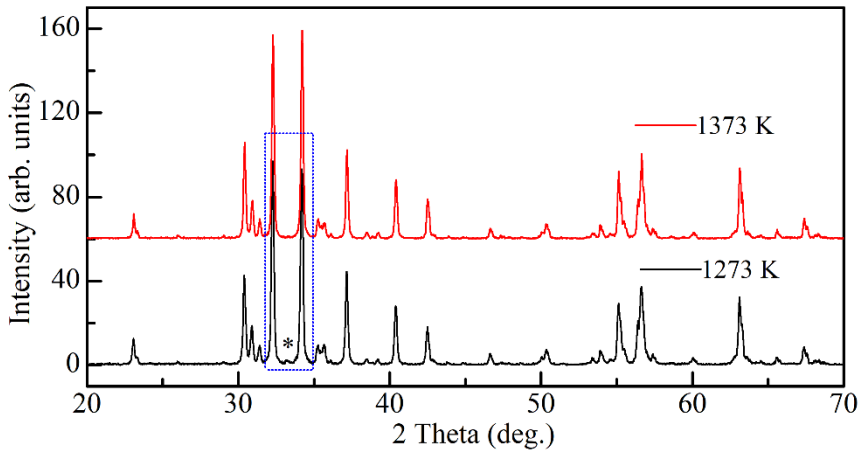

Figure 2.1: XRD profiles of $BaFe_{12}O_{19}$ calcined at 1273 K and 1373 K. The position of impurity peak due to Fe_2O_3 is marked with (*).

2.3.2 Optimization of Sintering Temperature

A few drops of 2% Polyvinyl Alcohol (PVA) solution in water was added to the calcined powder and mixed using a mortar and pestle. Pellets were made at an optimized load of 90 kN using a cylindrical steel die of 13 mm diameter on a uniaxial hydraulic press machine. After the palletisation, pellets were kept at 873 K for 10 hours so that the binder (PVA) is burnt off properly. To optimise the sintering temperature, the green pellets were sintered at different temperatures (1473 K, 1523 K and 1573 K) for 6 hours. The sintered pellets were crushed into fine powders and then annealed at 873 K for 10 hours before recording the XRD patterns which are shown in Fig. 2.2. The XRD patterns clearly show that the powder obtained from the pellets sintered at 1473 K and 1523 K remain monophasic. On the other hand, sample sintered at 1573 K shows one extra peak in the XRD pattern due to degradation. To be on the safe side, we sintered all the pellets at 1473 K for 6 hours. The experimental density of the sintered pellets was found ~ 96% of the theoretical density.

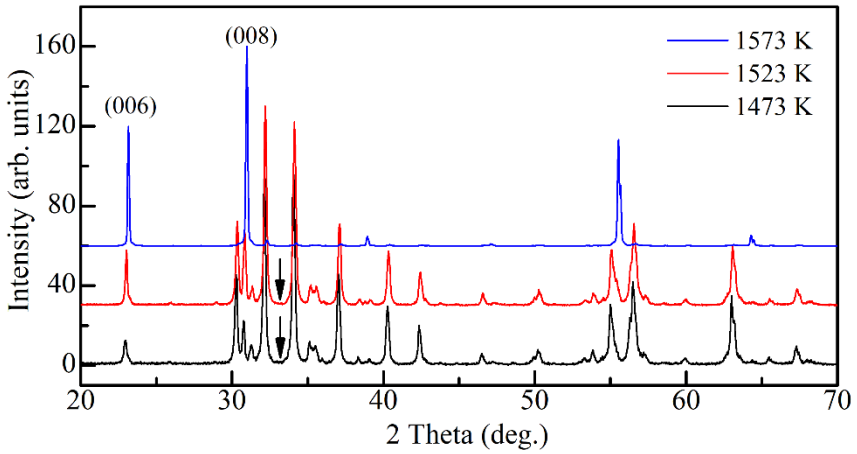

Figure 2.2: XRD profile for $BaFe_{12}O_{19}$, sintered at different temperatures. The position of the impurity peak of Fe_2O_3 is marked with arrow.

2.4 Details of Crystal Growth of $BaFe_{12}O_{19}$

The single crystals of BFO were grown using conventional high-temperature flux method with Na_2CO_3 flux [178,179]. For this, the as-calcined powder was mixed with Na_2CO_3 in the 80:20wt % ratio. This mixture was heated in a closed platinum crucible upto 1533 K at a heating a rate 5 K/min. The temperature was maintained at 1533 K for 5 hours for homogenization. After that, the crucible with molten material was cooled down to 1173 K at a rate of 4.5 K per hour. After reaching 1173 K, the crucible was left to cool down to room temperature in air. The crystals of BFO were harvested from different parts of the crucible. These single crystals were rinsed in warm dilute nitric acid to remove the flux sticking to the surface of the crystals.

2.4.1 Crystallinity and Phase Purity of Single Crystals

The as-grown crystals of BFO exhibit hexagonal platelet shape as can be seen from Fig. 2.3(a) which depicts the image of one such single-crystal. The sample crystallinity and symmetry were checked using Laue diffraction technique. The Laue pattern of a BFO single-crystal is shown in Fig. 2.3(b). The Laue pattern was recorded in the reflection geometry using a polychromatic beam incident along the c-axis of the unit cell. The presence of closely spaced diffraction spots along six symmetry related directions not only confirm the crystallinity but also confirm the hexagonal symmetry of the as-grown crystals.

To verify the phase purity of the as-grown crystals, we have crushed the crystals into fine powders and then annealed at 873 K for 10 hours. The XRD pattern recorded on such annealed samples is shown in Fig. 2.4. For comparison, we have also shown the XRD pattern of the as-calcined powder sample of BFO in the same figure. There is no evidence for the common impurity phase α-Fe_2O_3, whose most intense peak occurs at 2θ =

33.2^0 [189], in the XRD pattern. Thus, both the crystalline nature and phase purity of the crystal was confirmed by XRD studies.

Further, we also compared our XRD pattern on annealed powder samples obtained after crushing the sintered samples and single crystals with NPD pattern recorded on annealed powder samples obtained from the sintered sample of BFO (see Fig. 2.5).

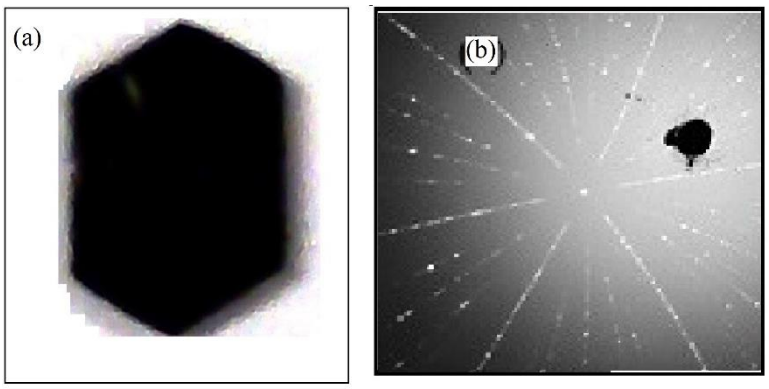

Figure 2.3: (a) Image of the as-grown crystal and (b) Laue diffraction recorded on the single-crystal of $BaFe_{12}O_{19}$.

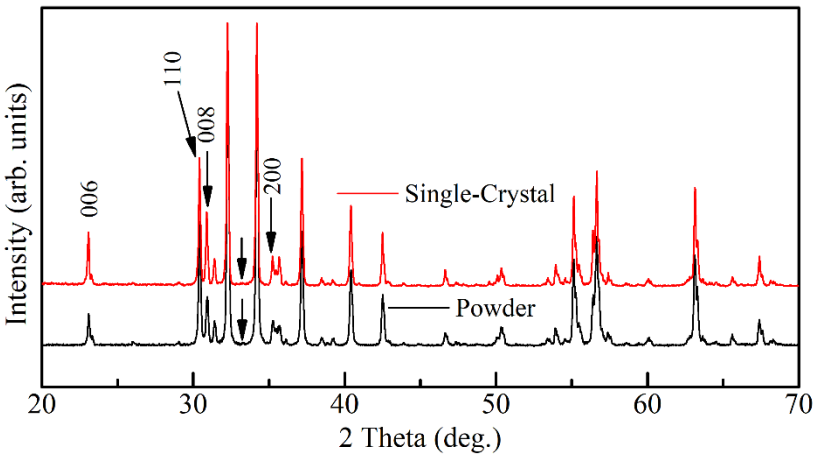

Figure 2.4: Comparison of XRD pattern on powder obtained after crushing the single-crystals and sintered samples of $BaFe_{12}O_{19}$. The arow shows the position of the most intense peak of α-Fe_2O_3 which is absent in both the samples.

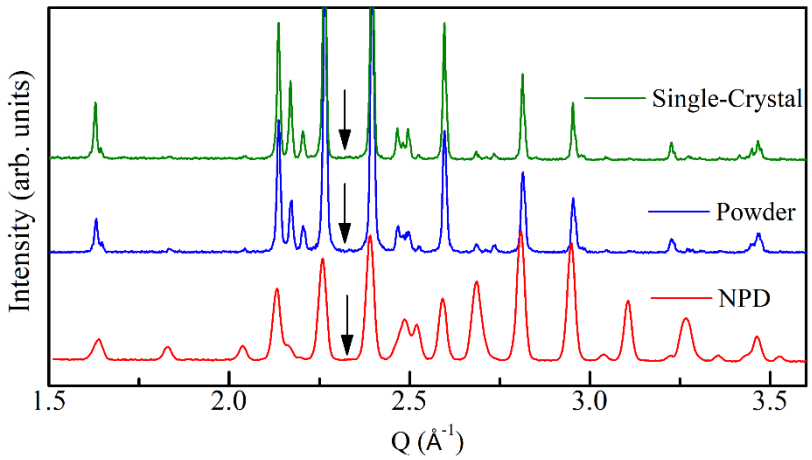

Figure 2.5: Comparison of neutron powder diffraction (NPD) pattern collected on sintered samples with XRD pattern collected on powder obtained after crushing the single-crystals and sintered samples of $BaFe_{12}O_{19}$, at room temperature. The Q = 2.32 $Å^{-1}$ marked with arrow is the position of most intense nuclear peak of α-Fe_2O_3 at 300 K.

It is evident from Fig. 2.5 that NPD also does not show any evidence of α-Fe_2O_3 impurity phase as its most intense nuclear peak at Q ~ 2.32 $Å^{-1}$ is absent in all the patterns. Thus, the XRD and neutron diffraction patterns of power and single-crystal samples confirm the monophasic nature of the polycrystalline and as-grown crystals of BFO.

2.4.2 Chemical Composition of Single Crystals

To check the chemical homogeneity, energy dispersive x-ray (EDX) spectra of the single crystals were recorded and a representative spectrum is shown in Fig. 2.6. This spectrum contains peaks corresponding to Ba, Fe and O only. Analysis of the EDX spectra after averaging over different regions of one such single-crystal is given in Table 2.1. It is evident that the atomic wt.% of Ba and Fe obtained by EDX analysis are close to the nominal compositions. Oxygen was excluded in the analysis as this technique is not sensitive enough for determining the content of low Z elements like O. The results of EDX analysis confirms Ba and Fe stoichiometry of the crystals and absence of any impurity element within the limit of EDX sensitivity.

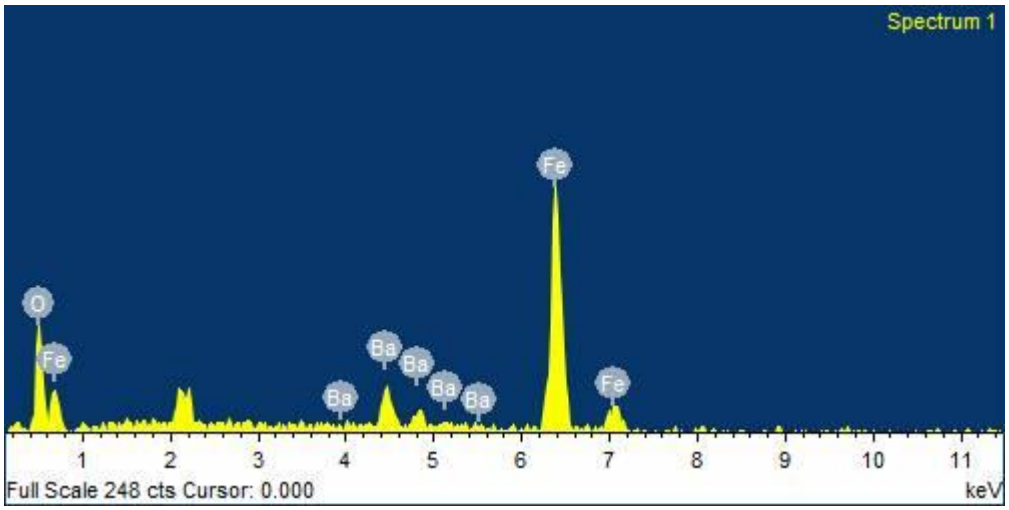

Figure 2.6: EDX spectra of single-crystal of $BaFe_{12}O_{19}$.

Table 2.1: Average chemical composition of $BaFe_{12}O_{19}$ in atomic wt% obtained from the EDX analysis.

Atoms	Atomic wt.% (As per formula)	Atomic wt.% (From the EDX)
Ba	7.69	7.7 ± 0.7
Fe	92.31	92.3 ± 0.7

2.4.3 Iodometry Titration

The oxygen content in BFO was determined using Iodometry titration method. To do the titration, powder sample of BFO (~ 15 mg) was dissolved in HCl (~ 10 ml). Potassium iodide (KI) (~ 1.2 times the weight of BFO) was added to the sample solution. In the final solution, I_2 is liberated through the following reaction.

$$2Fe^{3+} + 2I^{-} \rightarrow Fe^{2+} + I_2,$$

Few drops of starch solution were added to the sample solution to confirm the presence of I_2. The amount of I_2 in the solution is related to the number of Fe^{3+} ion in the same solution. The amount of Fe^{3+} ions can therefore be estimated by estimating the liberated I_2. To do this, the sample solution was taken in a 50 ml burate and titrated with 0.1 M of standard sodium thiosulfate ($Na_2S_2O_3$) solution. During the titration, following reaction takes place.

$$I_2 + 2Na_2S_2O_3 \rightarrow 2NaI + Na_2S_4O_6,$$

The end point of the titration was detected using starch-indicator. The oxygen content determined using this method was found to be 19 ± 0.2 for $BaFe_{12}O_{19}$.

2.5 Room Temperature Crystal Structure of $BaFe_{12}O_{19}$

BFO is an isomorphous compound of magnetic mineral magnetoplumbite $PbFe_{7.5}Mn_{3.5}Al_{0.5}Ti_{0.5}O_{19}$ with hexagonal crystal structure [12,118,119]. Our qualitative analysis using diffraction patterns confirm the monophasic nature of our synthesised polycrystalline and single-crystal samples of BFO. The magnetoplumbite structure with $P6_3/mmc$ space group of the as-calcined powder and single-crystal samples of BFO was confirmed by Rietveld technique using XRD data. During the refinement, the background was modelled using a six^{th}-order polynomial while the peak shape was modelled using pseudo-Voigt function. The Full-Width at Half-Maxima (FWHM) of the peaks were modelled using Caglioti equation [190,191]: $(FWHM)^2 = U\tan^2\theta + V\tan\theta + W$, where U, V and W are fitting parameters while θ is the Bragg peak. During the refinement, scale factor, zero displacement, lattice parameters, positional coordinates and thermal parameters were allowed to vary while the occupancy of each ion was fixed at their nominal composition value. The atomic coordinates of the asymmetric unit of the hexagonal cell with space groups $P6_3/mmc$ of $BaFe_{12}O_{19}$ are given in Table 2.2 [118].

The initial input parameters (structural and thermal) were taken from ref. [118]. The refinement converged satisfactorily after a few cycles. The observed and calculated profiles obtained after Rietveld refinement for both the samples are in excellent agreement as can be seen from Fig. 2.7 which depicts the fits in a limited 2θ range on a magnified scale. This confirms the magnetoplumbite structure of the as-calcined power and single-crystal samples with the $P6_3/mmc$ space group. The structural parameters, thermal parameter, agreement factors and χ^2 for the powder and single-crystal samples are listed in Tables 2.3 and 2.4, respectively. The refined lattice parameters and the structural parameters are in excellent agreement with those reported in the literature using single-crystal neutron and the x-ray diffraction studies [15,119,192], as can be seen from Table 2.5. The nearest-neighbour interatomic distances, obtained from the refined coordinates using Bond_Str program of FullProf suite [186], are listed in Table 2.6.

Table 2.2: Asymmetric unit of the hexagonal phase of $BaFe_{12}O_{19}$ in space groups $P6_3/mmc$.

Atoms	Wyckoff Site	x	y	z
Ba	2d	2/3	1/3	0.25
Fe1	2a	0	0	0
Fe2	2b	0	0	0.25
Fe3	4f1($4f_{iv}$)	1/3	2/3	z
Fe4	4f1($4f_{vi}$)	1/3	2/3	z
Fe5	12k	x	2x	z
O1	4e	0	0	z
O2	4f	1/3	2/3	z
O3	6h	x	2x	0.25
O4	12k	x	2x	z
O5	12k	x	2x	z

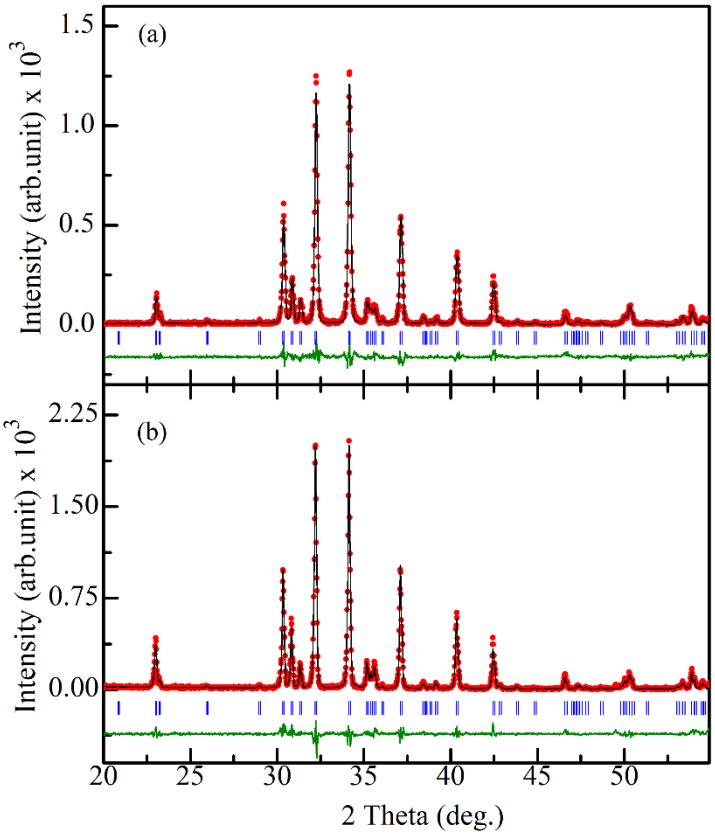

Figure 2.7: Observed (filled red circles), calculated (continuous black line), and difference (bottom green line) profiles obtained from Rietveld refinement using $P6_3/mmc$ space group for (a) powder and (b) single-crystal samples of $BaFe_{12}O_{19}$. The vertical bars (blue) represent the Bragg peak positions.

Table 2.3: Positional coordinates, lattice parameters, and agreement factors obtained by Rietveld refinement using powder XRD data of $BaFe_{12}O_{19}$.

Atoms/Coordinates	x	y	z	B
Ba	2/3	1/3	0.25	0.8(1)
Fe1	0	0	0	0.7(2)
Fe2	0	0	0.25	0.9(3)
Fe3	1/3	2/3	0.026(3)	0.8(2)
Fe4	1/3	2/3	0.189(3)	0.8(2)
Fe5	0.1731(8)	2x	-0.108(1)	0.0(1)
O1	0	0	0.15(1)	0.5(6)
O2	1/3	2/3	-0.04(1)	0.5(7)
O3	0.19(4)	2x	0.25	0.7(6)
O4	0.15(3)	2x	0.051(5)	0.1(4)
O5	0.49(3)	2x	0.149(6)	0.1(3)
$a = b = 5.890(1)$, $c = 23.186(8)$, $\alpha = \beta = 90$, $\gamma = 120$, $\chi^2 = 3.41$, $R_p = 15.5$, $R_{wp} = 30.0$, $R_{exp} = 16.2$				

Table 2.4: Positional coordinates, lattice parameters, and agreement factors obtained by Rietveld refinement using single-crystal XRD data of $BaFe_{12}O_{19}$

Atoms/Coordinates	x	y	z	B
Ba	2/3	1/3	0.25	0.842(1)
Fe1	0	0	0	0.674(3)
Fe2	0	0	0.25	0.899(3)
Fe3	1/3	2/3	0.02802(3)	0.850(2)
Fe4	1/3	2/3	0.19028(3)	0.846(2)
Fe5	0.17083(9)	2x	-0.10815(1)	0.422(1)
O1	0	0	0.14283(9)	0.211(7)
O2	1/3	2/3	-0.05354(8)	0.138(6)
O3	0.18797(3)	2x	0.25	0.375(5)
O4	0.15936(2)	2x	0.05350(5)	0.556(4)
O5	0.50094(2)	2x	0.14705(5)	0.513(4)
a=b= 5.888(1), c = 23.193(6), $\alpha = \beta = 90$, $\gamma = 120$, $\chi^2 = 1.91$, $R_p = 14.1$, $R_{wp} = 20.3$, $R_{exp} = 14.69$				

Table 2.5: Comparison of our structural parameters with those reported in literature using single-crystal data.

	A		B	C	D
Refined structural parameters	Our results		Single-crystal x-ray diffraction data (main text ref. [119]).	Single-crystal neutron diffraction data (ESI ref. [15])	Powder (obtained from crushing the single-crystals) neutron diffraction data (main text ref. [192])
	powder	Single-crystal			
a = b (Å)	5.890(1)	5.888(1)	5.8920(3)	5.8948(8)	5.80
c (Å)	23.186(8)	23.193(6)	23.183(1)	23.202(3)	23.18
z_{Fe3}	0.026(3)	0.02802(3)	0.02713(2)	0.02724(9)	0.0271
z_{Fe4}	0.189(3)	0.19028(3)	0.19030(2)	0.19031(9)	0.1902
z_{Fe5}	0.1731(8)	0.17083(9)	0.1686(8)	0.1688(3)	0.166(7)
z_{Fe5}	-0.108(1)	-0.10815(1)	-0.10825(1)	-0.10829(4)	-0.108(3)
z_{O1}	0.15(1)	0.14283(9)	0.15094(13)	0.15033(14)	0.149(7)
x_{O3}	0.19(4)	0.18797(3)	0.1821(3)	0.1818(7)	0.18(1)
x_{O4}	0.15(3)	0.15936(2)	0.1564(7)	0.1564(5)	0.16(20)
z_{O4}	0.051(5)	0.05350(5)	0.05192(8)	0.05204(8)	0.053(9)
z_{O5}	0.149(6)	0.14705(5)	0.14957(8)	0.14920(7)	0.14(80)

Table 2.6: Interatomic distances (Å) obtained from Rietveld refinement powder XRD data of $BaFe_{12}O_{19}$

Ba polyhedron		**Fe4 octahedron**	
Ba-O3	2.96(3)	Fe4-O3	2.00(3)
Ba-O5	2.90(2)	Fe4-O5	1.92(3)
Fe1 octahedron		**Fe5 octahedron**	
Fe1-O1	3.48(3)	Fe5-O1	2.019(1)
Fe1-O4	2.00(2)	Fe5-O2	2.126(1)
Fe2 trigonal bipyramid		Fe5-O4	2.14(2)
Fe2-O1	2.31(3)	Fe5-O5	3.49(2)
Fe2-O3	1.97(4)	Fe5-O5	1.937(2)
Fe3 tetrahedron		**Important distances**	
Fe3-O2	1.7793)	F5-Fe1	3.066(4)
Fe3-O2	3.442(4)	F5-Fe3	3.499(6)
Fe3-O4	1.878(2)	F5-Fe4	3.498(6)
Fe3-O4	3.46(2)	F5-Fe5	3.059(5)
Fe3-O5	3.229(2)	F5-Fe5	2.831(5)

2.6 Conclusions

BFO polycrystalline samples were synthesized successfully using conventional solid-state method. The phase purity was confirmed by XRD pattern. The single-crystal samples of BFO were grown successfully using high temperature flux method. The phase purity and crystallinity of the crystals were verified using XRD patterns, single-crystal neutron diffraction and Laue diffraction patterns. The composition of the crystals was confirmed using EDX technique and Iodometry titration method. The Rietveld refinement of the crystal structure of the as-calcined powder and powder obtained from the single crystals confirms the phase purity as well as the $P6_3/mmc$ space group of BFO. The refined structural parameters are in excellent agreement with those reported in the literature for polycrystalline and single crystals.